JOURNAL OF PROPULSION AND POWER
Vol. 13, No. 4, July–August 1997

Hydrogen Autoignition and Combustion in Supersonic Flow at Low Equivalence Ratio

Giulio Riva* and Giambattista Daminelli†
Consiglio Nazionale delle Ricerche, Peschiera Borromeo (Mi) 20068, Italy
and
Adolfo Reggiori‡
Università di Brescia, Via Branze, Brescia 25060, Italy

A supersonic high-enthalpy tunnel developed at CNPM–CNR to test hydrogen autoignition and combustion under simulated flight conditions in the high supersonic–low hypersonic range is capable of sustaining supersonic combustion for 10–30 ms, the flow residence time being about 1 ms. A simple but effective procedure for data analysis based on detailed static and total pressure measurements provides information on the one-dimensional quasisteady thermofluid-dynamic field inside the tunnel as a function of the upstream stagnation conditions. An efficient-mixing discrete-hole cross-stream injector was adopted, which also allowed hydrogen preheating. The equivalence ratio was limited to values ≤0.15 to keep the airstream supersonic in the constant cross-sectional portion of the tunnel. Autoignition delay data were obtained (0.1–1 ms) and correlated with the local static temperature. The results agree with experimental and theoretical literature data available for cold hydrogen. A strong effect of fuel temperature was observed, suggesting that a meaningful database for scramjet applications should always include, if appropriate, fuel preheating. Overall reaction times were also evaluated for different fuel temperatures, whose remarkable influence was confirmed.

Nomenclature

A	=	cross-sectional area, m^2
A/F	=	air/fuel mass ratio
b	=	tunnel width (along z axis), m
$E.R.$	=	equivalence ratio $(A/F)_{st,mass}/(A/F)_{mass}$
K	=	function depending on gas composition and temperature, Eq. (4)
M	=	Mach number
m	=	mass, kg
$\dot{m}$	=	mass flow, kg/s
p	=	pressure, Pa
R	=	gas constant, J/(kg K)
T	=	temperature, K
t	=	time, s
u	=	gas velocity, m/s
V	=	stagnation vessel volume, m^3
v	=	velocity, m/s
w	=	molecular weight, kg/mole
x	=	distance along the tunnel longitudinal axis (main flow direction), m
y	=	distance along the tunnel vertical axis, m
z	=	distance along the tunnel transversal axis, m
Δt	=	time interval, s
γ	=	specific heats ratio
ρ	=	density, kg/m^3

Subscripts

A	=	position A on the flame front, Fig. 4
air	=	air (without water vapor)
av	=	average
B	=	position B on the flame front, Fig. 4
C	=	position C on the flame front, Fig. 4
COMB	=	combustion
D	=	position D on the flame front, Fig. 4
E	=	position E on the flame front, Fig. 4
end	=	final
f	=	flame
H_2O	=	water vapor
H_2–O_2	=	hydrogen–oxygen stoichiometric mixture
i	=	location along x
ign	=	ignition
inj	=	injection
j	=	location along y
k	=	location along z
max	=	maximum
NO–COMB	=	noncombustion
re	=	reaction
st	=	stoichiometric
t	=	total
up	=	upstream
0	=	upstream stagnation vessel
1	=	before the shock wave produced by the injector assembly

Superscripts

$-$	=	average over one space
$=$	=	average over two spaces
$*$	=	throat

Introduction

HYDROGEN autoignition and combustion dynamics in high-enthalpy supersonic flows are major topics in the development of hypersonic flight propulsion systems. A number of studies have been published over several decades, providing a general overview of the research activity in this field, or focusing on some peculiar physical and technological features of the many complex phenomena involved. Development of the experimental facility employed in the present work took advantage of both these types of papers. Some of them were useful for defining the operating conditions[1,2] and the general

Received Oct. 30, 1995; revision received Feb. 2, 1997; accepted for publication Feb. 12, 1997.

*Research Scientist, CNPM, Viale Baracca 69.
†Research Assistant, CNPM, Viale Baracca 69.
‡Professor, Dipartimento di Ingegneria Meccanica.

channel geometry,[2,3] others gave indications about fuel-injection techniques and injector geometry.[4–7]

A common peculiarity of almost all the supersonic combustion test facilities is the contamination of the supersonic airstream caused by the products of precombustion, a commonly used technique to increase air stagnation enthalpy, often in combination with other energy addition techniques. Several papers were recently published on the effects of such contaminants (H_2O, OH, H, O, NO, ...) on the hydrogen ignition and combustion process[8–10] and, in some cases, a remarkable influence was observed.[10] In our case, however, pre-combustion products contents and thermodynamic conditions are kept to levels probably involving small influences from this viewpoint. Air contamination in test facilities for hypersonic flight Mach numbers less than 8 is, however, an open issue that needs further studies to be done.[1]

The experimental tests presented in this work refer to flight conditions typical of the high supersonic–low hypersonic range (M_∞ = 4–7). In this range it may be difficult to achieve sufficiently fast and stable ignition in supersonic combustors. These are also the only hypersonic flight conditions that can be studied in ground facilities of reasonably small size. Similar test conditions were also investigated in papers that provided a very useful database for comparing some of the results presented in this work.[3,4,5,11,12]

In this paper, hydrogen autoignition delay, overall reaction time, and minimum air total temperature required for ignition are compared for two hydrogen stagnation temperatures (i.e., 300 and 500 K) and an equivalence ratio up to 0.15.

Experimental Setup

A supersonic high-enthalpy tunnel has been developed at CNPM–CNR with the specific purpose to investigate mixing, ignition, and combustion characteristics of fuels injected in supersonic flow. Immediately downstream of the supersonic nozzle, the tunnel test section is of a constant rectangular cross sectional area (2.6 cm height, 3 cm width, 25 cm length). A rectangular cross-sectional area divergent follows (6 deg angle, 3 cm width, 60 cm length) (Fig. 1).

The tunnel is fed with high-enthalpy vitiated air coming from a 15-l free-piston compression tube (4 m length), in which the effects of rapid compression and hydrogen precombustion are combined to produce stagnation temperatures of about 2000–2500 K and pressure up to 5 MPa. These conditions are obtained inside a vessel that is fed by the piston-compressed air through a check valve. The high-enthalpy vitiated air is then expanded into the supersonic nozzle following the breakup of a calibrated diaphragm.

The experimental tests reported and analyzed in this paper were carried out with the injector placed in the constant area section of the tunnel, 10 cm before the beginning of the divergent. The injector assembly consisted of twin (downstream and upstream, 2 mm spacing) stainless-steel pipes, 2 mm external diameter, crossing the tunnel spanwise and placed midway with respect to the channel height (Fig. 2). The downstream pipe had 10 holes (2 rows of 5), 0.4 mm diam each, their axis at ±60 deg with respect to the horizontal symmetry plane. The hydrogen temperature was varied by electrically heating the pipe connecting the injector to the reservoir, whose volume was calibrated to keep the equivalence ratio constant during the whole injection period and for the two hydrogen temperatures tested. Because of the injector geometry and position the hydrogen was fed immediately behind the blunt shock generated by the upstream pipe. Flow conditions suitable for sustaining hydrogen self-ignition and combustion in supersonic flows can be maintained from 10 to 30 ms, the gas residence time being of the order of 1 ms.

Pressure along the tunnel was measured midway with respect to the channel height using transducers with 0.7 MPa full scale, 1 MHz natural frequency, ±1% global accuracy. The stagnation pressure (upstream air reservoir) was detected with a 14 MPa full-scale transducer with similar characteristics. A 12-bit resolution multichannel transient recorder was used for data acquisition.

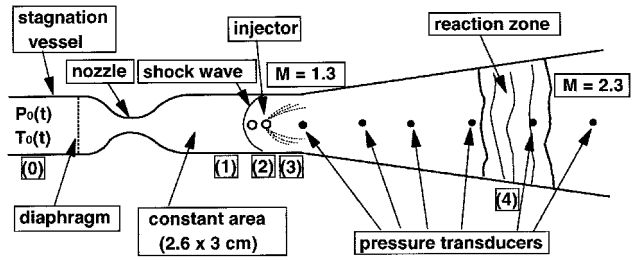

Fig. 1 Qualitative sketch of the supersonic tunnel.

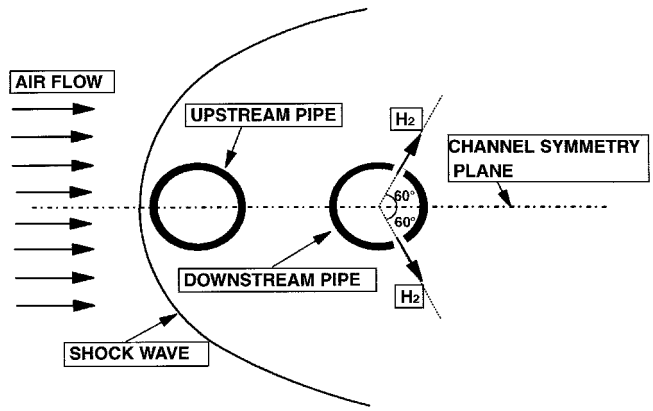

Fig. 2 Qualitative sketch of the injector structure.

Tunnel Calibration

The analysis of the combustion tests was made possible by a preliminary calibration, whose purpose was to provide a map in terms of pressure, temperature, and Mach number along the tunnel. In particular, this calibration established a correlation between upstream stagnation pressure (always measured) and upstream stagnation temperature. Based on this correlation, pressure measurements, and some simplifying assumptions, the thermal and fluid dynamic fields inside the tunnel could be determined with reasonable approximation. Static and total pressure measurements were used to evaluate the Mach number of the airflow immediately before the injection location ($\bar{M}$ = 2). Average values of pressure and Mach number were evaluated under three different flow conditions (combustion, fuel injection without combustion, no fuel injection) at five equally spaced axial stations along the divergent, on the basis of detailed static and total pressure maps detected over the five corresponding cross-sectional areas. For the unreacting flow condition the average Mach number was found to increase from 1.3 (injector position, behind the shock wave) to 2.3 (exhaust), with air velocity correspondingly going from 700 to 1100 m/s.

By assuming the divergent inlet as the origin of the abscissa (x = 0), the tunnel axial locations where average pressures were computed are placed at x = 0.06, 0.172, 0.285, 0.4, and 0.515 m. Static (wall) pressure was measured at each axial position at several different locations along the channel height (y direction). As expected, measurements of static spanwise pressure (along the z direction) indicated constant spanwise pressure; consequently, pressure was averaged taking into account the y distribution only.

Along the divergent, local values of the Mach number were computed from pitot and static pressure measurements at each axial location, and several positions along the y direction, on the midplane with respect to the channel width. Since the Mach number distribution is fully three dimensional, pitot

pressures spanwise on the midplane with respect to the channel height were also measured. A probe with six equally spaced ($\Delta z = 2.5$ mm) sensors provided the spanwise Mach distribution along the channel (half) width. Symmetry with respect to the channel vertical midplane was assumed. Once the Mach number field was known, the average Mach at each cross section was computed as follows. First, the average Mach number along the y axis $\bar{M}_{i,k=1}$ was calculated using linear interpolation among the internal points and a parabolic distribution between walls and the nearest measurement location; the Mach values along the z axis were then used to scale the corresponding contributions to the average Mach:

$$\bar{\bar{M}}_i = \frac{\Delta z}{b}\,\bar{M}_{i,1}\left(1 + 2\sum_{k=2}^{6}\frac{M_{i,k}}{M_{i,1}}\right) \tag{1}$$

Procedure for Combustion Tests Analysis

The evaluation of gaseous hydrogen ignition delay and reaction times is based on the static pressure measurements downstream of the fuel injection structure. Other essential data are the upstream stagnation conditions (pressure, temperature, gas composition) and the flow conditions at the fuel injection location. The scheme of the tunnel in Fig. 1 shows the axial locations relevant to this analysis. Such locations are locations (0), upstream stagnation conditions, $p_0(t)$ known; (1), conditions immediately upstream of the fuel injection structure ($\bar{\bar{M}} = 2$); (2), conditions immediately downstream of the shock wave; (3), conditions after fuel injection (air/H_2 mass flow ratio is constant in time and known); and (4), flow conditions at ignition location, pressure and Mach number are known from experimental data.

Evaluation of the Upstream Stagnation Conditions (0)

The procedure for evaluating all of the relevant quantities at the locations just mentioned is the following. The pressure history inside the stagnation volume [position (0)] is known from measurements. The evaluation of temperature and gas composition is based on a calibration of the setup, carried out by keeping the high-enthalpy gas coming from the piston tube confined inside the vessel and measuring the whole pressure history, including the final pressure, when ambient temperature T_{end} is reached. The gas coming from the piston tube is the product of precombustion of a mixture of air (0.1 MPa) and a stoichiometric H_2–O_2 mixture produced by an electrolytic cell (0.0356 MPa). The simultaneous effect of compression and hydrogen pre-combustion produces the desired high-enthalpy conditions. Assuming a complete H_2 combustion and a complete water condensation as the final temperature ($T_{\text{end}} = 300$ K) is reached, a correlation between maximum stagnation pressure (measured) and maximum stagnation temperature can be derived:

$$T_{0,\max} = \frac{p_{0,\max}}{p_{\text{end}}}\frac{R_{\text{air}}}{R}\frac{T_{\text{end}}}{1 + \frac{2}{3}(p_{\text{H}_2\text{-O}_2}/p_{\text{air}})(w_{\text{H}_2\text{O}}/w_{\text{air}})} \tag{2}$$

The maximum temperature given by Eq. (2) as a function of the (measured) maximum pressure was obtained for a closed vessel. During a normal experimental test, the vessel fed by the piston tube is connected to the supersonic tunnel. This occurs, however, only after breakup of the diaphragm whose breakup pressure is slightly less than the maximum pressure. Moreover, the relatively small nozzle area makes the pressure history of actual supersonic combustion tests quite similar to that in the calibration tests, at least during the raising portion. Since the initial conditions and the operation of the piston tube are identical in the two cases, Eq. (2) can reasonably be applied to supersonic combustion tests, giving with acceptable accuracy the maximum stagnation temperature. Such a temperature is fundamental for scaling the whole temperature field inside the supersonic tunnel as a function of time. In practical terms, the calibration tests provided the final pressure p_{end} inside the (closed) vessel as a function of the percentage of H_2–O_2 stoichiometric mixture. The value corresponding to the initial conditions adopted in all of the combustion tests inside the free piston compression tube is 0.47 MPa, which is the only quantity taken from calibration tests needed in the procedure detailed earlier. At this stage, pressure history $p_0(t)$, gas composition, and maximum temperature are known at the location (0); however, the time history of temperature still has to be determined. Mass conservation, coupled with state equation and the assumption of adiabatic and isentropic flow along the convergent portion of the supersonic nozzle, lead to the following expression of the stagnation temperature as a function of time:

$$T_0(t) = T_{0,\max}\exp\left\{\ell n\left[\frac{p_0(t)}{p_{0,\max}}\right] + \int_{t(T_{0,\max})}^{t} K\sqrt{T_0(t)}\,\mathrm{d}t\right\} \tag{3}$$

where

$$K = \frac{A^*}{V}\left(\frac{2}{\gamma + 1}\right)^{[(\gamma+1)/2(\gamma-1)]}\sqrt{\gamma R} \tag{4}$$

Equation (3) can easily be solved iteratively, providing the upstream stagnation conditions as a function of time. Then the correct upstream conditions at any time of interest can be computed (e.g., every time the combustion wave is detected by any of the pressure transducers along the divergent channel).

Evaluation of Conditions (1) Immediately Before the Injector

A preliminary number of calibration experiments gave the average Mach number at this axial location as $\bar{\bar{M}} = 2$. Continuity equation, coupled with the measurement of the local static pressure and Mach number can be used to compute all of the other relevant quantities (temperature, gas speed, . . .). In this case the static pressure measured on the horizontal midplane with respect to the channel height was used. On the basis of this experimental information, the continuity equation can predict the static temperature

$$T_1(t) = \frac{\gamma_1}{R_1}\left[\frac{\bar{p}_1(t)\bar{\bar{M}}_1 A_1}{\dot{m}_1(t)}\right]^2 \tag{5}$$

where

$$\dot{m}_1(t) = \dot{m}_0(t) = \frac{p_0(t)}{\sqrt{T_0(t)}}\left(\frac{2}{\gamma + 1}\right)^{[(\gamma+1)/2(\gamma-1)]} A^*\sqrt{\frac{\gamma}{R}} \tag{6}$$

Once $T_1(t)$ is known, all other relevant quantities can be computed in a straightforward manner.

Evaluation of Flow Conditions (2) Behind the Shock Wave

The injector assembly produces a shock wave that is normal near the channel midplane and oblique (with decreasing angle) between the midplane and the horizontal walls. To simplify the treatment, an equivalent oblique two-dimensional shock has been assumed to replace the true shock. Its angle has been determined by two-dimensional calculations applied to flow conditions consistent with those existing at location (2) of the channel. The oblique shock equations thus provide the nominal conditions at the fuel injection location. It is worth stressing that the flow properties computed according to this procedure are average values over the cross-sectional area, and their use in analyzing the data must take into account that locally variations may exist around their average levels.

Evaluation of Flow Conditions (3) After Fuel Injection

The equivalence ratio is constant and known during the whole injection period. Thus, average properties of the hydrogen-vitiated air mixture can be calculated. Since very low *E.R.* (0.15 or less) were tested, average pressure, temperature, and speed of the airstream experience minor changes.

Evaluation of Flow Conditions at Ignition Location (4)

At the ignition location, average pressure and Mach numbers are known from experimental data (if needed, interpolation is performed). Mass conservation gives the total mass flow rate as the sum of the airstream and hydrogen contribution. As done for location (2), the static temperature can be computed using the continuity equation and the other relevant quantities are then immediately computed.

Ignition Delay and Reaction Time

Hydrogen combustion tests were performed for *E.R.* = 0.05, 0.1, and 0.15, and for hydrogen stagnation temperatures 300 and 500 K at the start of injection. Injector geometry and position were kept constant. The *E.R.* had to be limited to such low values to keep the flow supersonic in the constant area portion of the duct (except in the unavoidable small subsonic region inside the injector wake). Higher values of the *E.R.* could be obtained without transitioning to subsonic flow by either decreasing the angle of the holes feeding the hydrogen or by moving the injector closer to the divergent. In these tests the following measurements were performed: total pressure inside the upstream vessel, total pressure inside the hydrogen reservoir, and static pressure at several locations along the supersonic tunnel.

The time of transit of the combustion wave in front of the monitoring stations downstream of the fuel injector was detected and correlated to the instantaneous upstream stagnation pressure. The preliminary calibration then provided the corresponding upstream total temperature [Eq. (3)] and the procedure summarized in the previous section gave the one-dimensional thermofluid-dynamic field inside the tunnel. In other words, at each pressure-monitoring station downstream of the injector, a quasisteady combustion configuration could be analyzed. A meaningful and immediately readable picture can be obtained by showing the ratio static/upstream total pressure at the measurement locations vs time. A typical example is given in Fig. 3, where the curves refer to axial stations 9.8, 17.7, 23.3, 34.7, 46.1, and 57.7 cm, respectively, downstream of the injector position, covering the whole divergent.

Using the experimental data (Fig. 3), the time at which the combustion wave is assumed to be at a certain axial location

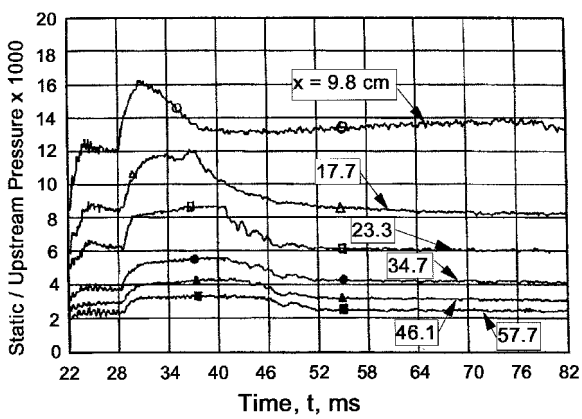

Fig. 3 Example of static/upstream pressure traces vs time at different monitoring locations along the divergent (cold hydrogen, *E.R.* = 0.15).

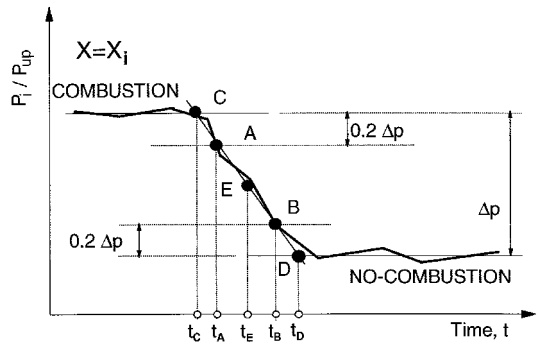

Fig. 4 Sketch showing the reaction zone characterization criteria.

(i.e., at each of the pressure measurement points) can be evaluated. To be more consistent, it is necessary to establish which point of the combustion wave should be chosen to define its position. In fact, especially under relatively low air temperature conditions, the wave thickness may be comparable to the tunnel length. The criteria adopted to characterize the flame front are summarized in Fig. 4. Consider first the average values of the pressure ratio for the two cases of combustion and no-combustion and define

$$\Delta p_i = \overline{(p/p_{t,\mathrm{up}})}_{i,\mathrm{COMB}} - \overline{(p/p_{t,\mathrm{up}})}_{i,\mathrm{NO\text{-}COMB}} \tag{7}$$

Let us define points (A) and (B) as follows:

$$(A) \rightarrow \overline{(p/p_{t,\mathrm{up}})}_{i,\mathrm{COMB}} - 0.2\Delta p_i \tag{8}$$

$$(B) \rightarrow \overline{(p/p_{t,\mathrm{up}})}_{i,\mathrm{NO\text{-}COMB}} + 0.2\Delta p_i \tag{9}$$

The straight line passing through these two points crosses the lines representing the combustion and no-combustion average pressure values at points (C) and (D). Eventually, at each pressure-monitoring location i, we can define the following quantities:

$$\Delta t_{f,i} = t_D - t_C \tag{10}$$

$$t_{f,i} = t_E = (t_D + t_C)/2 \tag{11}$$

$$t_{\mathrm{ign},i} = t_D \tag{12}$$

The physical meaning of the quantities given previously is $\Delta t_{f,i}$, total transit time interval of the combustion wave across the monitoring location x_i; $t_{f,i}$, time of transit of the combustion wave midpoint at monitoring location x_i; and $t_{\mathrm{ign},i}$, time of transit of the conventional ignition point at monitoring location x_i.

The ignition delay is evaluated according to the following procedure: 1) the conventional ignition time given by Eq. (12) is assumed; 2) the corresponding value of the upstream stagnation pressure is identified; and 3) using the procedure of the previous section, the one-dimensional quasisteady thermofluid-dynamic field along the tunnel is determined and, in particular, the flow velocities at injection location x_{inj} and monitoring location x_i are evaluated and the average value $\bar{u}_{\mathrm{inj},i}$ is computed. The ignition delay can eventually be computed as

$$\Delta t_{\mathrm{ign}} = (x_i - x_{\mathrm{inj}})/\bar{u}_{\mathrm{inj},i} \tag{13}$$

One further problem is to decide which temperature such a ignition delay has to be correlated with. Two possible choices can either be the temperature at the fuel injection point or an average temperature, computed taking into account both injection and monitoring location values. The plots reported in Figs. 5 and 6 present both of these possibilities.

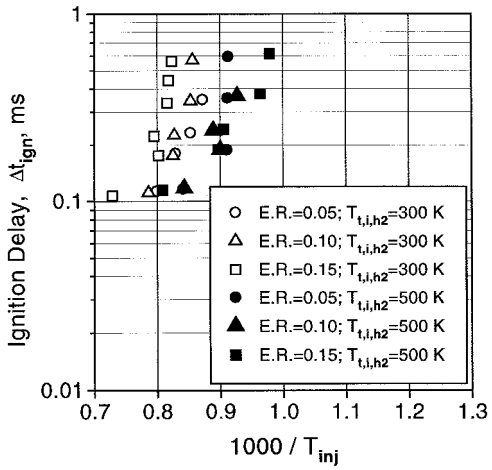

Fig. 5 Ignition delay as a function of air temperature at the injection location for different values of *E.R.* and hydrogen injection temperature.

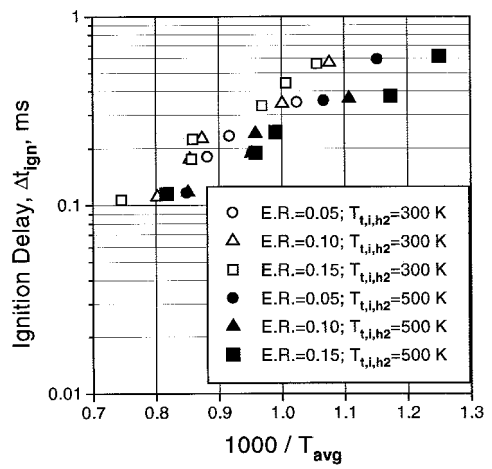

Fig. 6 Ignition delay as a function of the average temperature between injection location and flame position for different values of *E.R.* and hydrogen injection temperature.

The ignition delay results shown in Figs. 5 and 6 point out the importance of fuel preheating. In fact, despite the relatively small hydrogen temperature increment (about 200 K), the effect is remarkable and systematic. Ignition delays determined by chemical kinetic considerations are available in literature.[8,9] Typical values are in the range 0.1–1 ms for pressures and temperatures of concern in scramjet applications. Such data refer to premixed mixtures, often with *E.R.* close to unity and, at least in principle, should provide lower temperature boundaries for nonpremixed combustion. In real supersonic combustors, however, local temperature may be much higher than mean airstream values (especially when cross-stream injectors are present), making autoignition possible at lower mean temperatures.[2] The pressure dependence of hydrogen autoignition is also relevant. For example, at T = 750 K, ignition delay times controlled by chemical kinetics decrease from 1 to 0.1 ms by increasing pressure from 0.01 to 0.1 Mpa (Ref. 8). The present data refer to pressure levels that decrease as the temperature decreases. For example, Fig. 5 gives ignition delay as a function of the temperature at injection location, where the pressure, for the temperature interval of concern, covers the range 0.08–0.04 MPa. A further extension of the pressure range toward lower values, because of the flow expansion along the divergent, has to be considered if ignition delay is given as a function of an injector-flame position average temperature, as done in Fig. 6. In this case the lower boundary of the pressure range may be as low as 0.02 MPa. It has to be

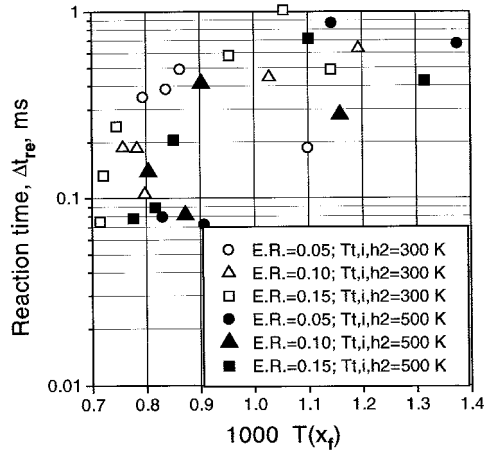

Fig. 7 Reaction time as a function of temperature at the flame location.

remarked that, under high-temperature conditions (fast chemical kinetics), the time required for mixing prevents ignition delay from reducing below a threshold of about 100 μs.

During the combustion tests, the reaction wave moves progressively downstream since, because of the temperature decrease following the discharge from reservoir, ignition delay becomes longer and, consequently, the distance of the ignition point from the fuel injector increases. The flame velocity with respect to the tunnel walls depends essentially on the rate of temperature decrease. The flame speed can be calculated along the tunnel as x_i and $t_{f,i}$ are known. The next step is the definition of the flame thickness:

$$\Delta x_{f,i} = v_{f,i}\Delta t_{f,i} \tag{14}$$

The total reaction time is defined as the residence time of the gas inside the flame region whose thickness is defined by Eq. (14). At each monitoring location i we can write

$$\Delta t_{re,i} = \Delta x_{f,i}/(\bar{u}_{g,i} - v_{f,i}) \tag{15}$$

Reaction times are reported in Fig. 7 as a function of the temperature at the pressure-monitoring locations. It must be stressed that all of the results reported in this work refer to quasisteady situations, in which the flame speed with respect to the tunnel walls is much lower than the gas speed (one order of magnitude at least).

Minimum Temperature Required for Ignition

During the discharge from reservoir, both pressure and temperature decrease in time. As a consequence, ignition delay is lengthened and thus the flame progressively approaches the tunnel exit. The limit configuration in which the ignition point coincides with the last pressure monitoring location can be regarded as a lower boundary for ignition. In fact, under such a condition, the flow temperature decrease is relatively low, while the temperature sensitivity of the ignition process is high. This situation, which can reasonably be considered very close to the ignition limit, is summarized in Fig. 8, where the ignition limit is given as a function of the upstream total temperature.

Figure 8 clearly shows the remarkable effect of the hydrogen temperature, whose increase lowers the ignition limit. Raising the *E.R.* also lowers the temperature needed for ignition, but this effect seems to be balanced by the local cooling when hydrogen is cold. As pointed out by Kinzei et al.[4] and Sato et al.,[11] autoignition in a supersonic flow of cold hydrogen is not expected for stagnation temperatures below 1500 K. The effectiveness of hydrogen preheating in lowering such a threshold value is made evident in Fig. 8. Moreover, the benefit

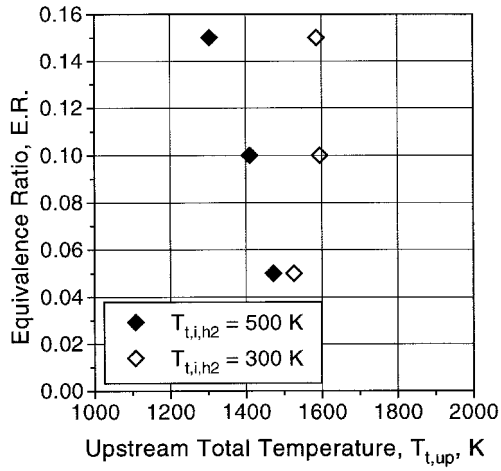

Fig. 8 Minimum upstream air stagnation temperature required for ignition: effect of *E.R.* and hydrogen stagnation temperature.

increases as *E.R.* increases, at least for the range investigated. Since fuel preheating is one of the suggested mechanisms for cooling hypersonic vehicles surfaces,[2] the usefulness of data in this area would greatly be enhanced if fuel preheating was systematically adopted during experimental tests in ground facilities.

Conclusions

Hydrogen autoignition delay and reaction times in high-enthalpy supersonic airflow were obtained as functions of the air static temperature. Two hydrogen stagnation temperatures (300 and 500 K) and three *E.R.* (0.05, 0.1, and 0.15) were explored. Ignition delay-time reductions ranging from 20 to 60% were found, depending on the airstream static temperature, by increasing the hydrogen stagnation temperature. Similar but less systematic effects of the hydrogen preheating were observed on the reaction time. The minimum air stagnation temperature required for hydrogen autoignition significantly decreases raising the hydrogen temperature. This effect is enhanced at higher *E.R.*, in particular, air stagnation temperature reductions ranging from 6% (*E.R.* = 0.05) to 18% (*E.R.* = 0.15) were found.

References

[1]Bushnell, D. M., "Mixing and Combustion Issues in Hypersonic Air-Breathing Propulsion," *Combustion in High Speed Flows, ICASE/LaRC Interdisciplinary Series in Science and Engineering*, edited by J. Bookman, T. L. Jackson, and A. Kumar, Kluwer, Dordrecht, The Netherlands, 1994, pp. 3–16.

[2]Billig, F. S., "Research on Supersonic Combustion," *Journal of Propulsion and Power*, Vol. 9, No. 4, 1993, pp. 499–514.

[3]Northam, G. B., Capriotti, D. P., Byington, C. S., and Greensberg, I., "Supersonic Mixing and Combustion in Scramjets," 10th International Symposium on Air Breathing Engines, Paper 91-7095, Nottingham, England, UK, Sept. 1991.

[4]Kinzei, N., Komuro, T., Kudou, K., Murakami, A., Tani, K., Masuya, G., and Wakamatsu, Y., "Effects of Injector Geometry on Scramjet Combustor Performance," 10th International Symposium on Air Breathing Engines, Paper 91-7132, Nottingham, England, UK, Sept. 1991.

[5]Komuro, T., Wakamatsu, Y., Murakami, A., Kudou, K., Tani, K., Masuya, G., Yamaoka, Y., Ninomiya, K., Kosaka, K., and Shinozaki, N., "Combustion Tests and Thermal Analysis of Fuel Injection Struts of a Scramjet Combustor," 10th International Symposium on Air Breathing Engines, Paper 91-7133, Nottingham, England, UK, Sept. 1991.

[6]Bogdanoff, D. W., "Advanced Injection and Mixing Techniques for Scramjet Combustors," *Journal of Propulsion and Power*, Vol. 10, No. 2, 1994, pp. 183–190.

[7]Lee, J., "Numerical Study of Mixing in Supersonic Combustors with Hypermixing Injectors," *Journal of Propulsion and Power*, Vol. 10, No. 3, 1994, pp. 297–304.

[8]Mitani, T., "Ignition Problems in Scramjet Testing," *Combustion and Flame*, Vol. 101, No. 3, 1995, pp. 347–359.

[9]Golovitchev, V. I., and Bruno, C., "Modeling of Parallel Injection Supersonic Combustion," *Proceedings of the 19th ISTS*, edited by M. Hinada, AGNE Shafu Publishing, Inc., Tokyo, 1994.

[10]Morgan, R. G., Stalker, R. J., Bakos, R. J., Tamagno, J., and Erdos, J. I., "Scramjet Testing—Ground Facility Comparison," 10th International Symposium on Air Breathing Engines, Paper 91-194(L), Nottingham, England, UK, Sept. 1991.

[11]Sato, Y., Sayama, M., Masuya, G., Komuro, T., Kudou, K., Murakami, A., Tani, K., and Chinzei, N., "Experimental Study on Autoignition in a Scramjet Combustor," *Journal of Propulsion and Power*, Vol. 7, No. 5, 1991, pp. 657, 658.

[12]Tomioka, S., Nagata, H., Segawa, D., Ujiie, Y., and Kono, M., "Effect of Combustion on Mixing Process in a Supersonic Combustor," 10th International Symposium on Air Breathing Engines, Paper 91-7094, Nottingham, England, UK, Sept. 1991.